Solid-State Dynamic Nuclear Polarization for Materials Study

Fabien AUSSENAC, Melanie ROSAY†
Bruker BioSpin

Summary

Solid-state Nuclear Magnetic Resonance (ssNMR) provides unique structural and dynamical information of materials at a molecular level. However, the low sensitivity of NMR is a major limitation for the detection of materials interfaces, dilute species and insensitive nuclei (^{17}O, ^{43}Ca, etc.). In this context, Dynamic Nuclear Polarization (DNP), a method to hyperpolarize nuclear spins, can enhances NMR sensitivity by several orders of magnitude. The solid-state DNP approach provides otherwise inaccessible structural and dynamical insights into a broad variety of materials, including organic, inorganic, bio-materials and hybrid systems.

Introduction

Solid-state NMR is a powerful spectroscopic technique offering unique information on the structure and dynamics of materials at a molecular scale. It is frequently used to characterize various materials for applications in energy storage, catalyst, health (e.g., drug delivery, bio-materials), construction and transportation. As a non-invasive method with atomic-scale resolution, ssNMR is especially suited to provide detail, and explore or define a variety of physical states that may be critical to function: amorphous (e.g., in polymers, glasses), disorder (in battery materials), soft (in liquid crystals, gels, pastes) or heterogeneous (in catalyst, nanomaterials). It can also distinguish

and quantify mixtures of states, for example, as sometimes present in pharmaceutical formulations. However, ssNMR suffers from low sensitivity of detection due to the weak magnetization (polarization) of nuclear spins at thermal equilibrium. This has been a major limitation in solving important questions for materials science, such as the study of surfaces and interfaces, low concentration, or diluted samples, and for observation of low natural abundance or low-gamma nuclei (^{17}O, ^{15}N, ^{43}Ca, ^{89}Y, etc.), which are still more weakly polarized than the most accessible nuclei, like ^1H, ^{19}F, ^{31}P or even ^{13}C).

Different strategies have been developed to boost the NMR sensitivity. One of the most powerful is Dynamic Nuclear Polarization (DNP), which hyperpolarizes nuclear spin magnetization to increase the signal intensity in NMR by factors of 10 to a few hundred. The basic principle of DNP is to transfer the high electron spin polarization from an admixed molecular radical (or similar source of unpaired electrons) to surrounding nuclear spins. This is achieved by sample irradiation at a frequency close to the EPR transitions (EPR: Electron Paramagnetic Resonance). The material of interest is typically mixed with a solvent containing the radicals, then Magic Angle Spinning (MAS) NMR experiments are performed on the frozen sample at high magnetic field (400, 600, 800 or 900 MHz ^1H NMR frequencies) and low temperature (ca. 100 K). Various sources (most often gyrotrons or klystrons) are used for microwave (MW) irradiation of typically 1 - 10 W at appropriate frequency

(see details below in the section on solid-state DNP instrumentation). The solid-state DNP approach enables ssNMR experiments, including multi-dimensional, which otherwise may have been impossible because of sensitivity limitations. This opens a new avenue to obtain structural and dynamical insights into materials[1].

In this application note, we discuss the preparation of material samples for DNP measurements. The DNP instrumentation is also briefly described. Finally, a selection of examples of DNP applications is presented for the characterization of different types of materials.

Preparation of materials samples

Sample preparation is often the most critical step for the success of DNP measurements. In this section, we describe approaches targeted on materials samples. Iterative preparations, varying parameters discussed below, may be required to optimize NMR sensitivity.

Generally, four different method families are explored to introduce a polarizing agent (i.e., the radical) into the material of interest.

1) Glass forming: sample is dissolved in a glass-forming solvent (e.g., water/glycerol) containing the radical, where glassing avoids radical aggregation and ensures homogeneous distribution throughout the final bulk frozen solution,

2) Film-casting: sample is dissolved in a radical solution, then solvent is evaporated off leaving a film of well-mixed sample plus radical,

3) Porous impregnation: a porous material sample is impregnated with the radical solution[2] (e.g., by pipetting) and the wetted or pasty product is used for DNP

4) Non-porous impregnation: a non-porous material is handled in similarly manner as the porous method, but here resulting in a sample where the radical solution wets the material surface (Figure 1).

Either aqueous or organic solvents can be used for each of the above, appropriate of course to both the material and the chosen radical. For materials, halogenated organic solvents, e.g., Tetrachloroethane (TCE), often give the highest DNP enhancement factor[3]. Solvents containing protonated methyl groups must be avoided as they produce poor DNP gain due to fast methyl rotations that survive at low temperature and contribute significantly to fast electron and nuclear spin relaxation times. It is also valuable degas organic solvents in order to remove the paramagnetic molecular oxygen (O_2)[4], which also contributes to excessive nuclear and electron relaxation rates and, without removal, tends to diminish DNP performance. In some cases, the materials themselves have high affinity to O_2, such as polymer with aromatic groups. In these cases, de-oxygenation treatment is of similar value[5].

So far, the most efficient polarizing agents for the Cross Effect (CE) DNP mechanism[6] at a temperature of 100 K are bi-nitroxide radicals. AMUPol[7] is a water-soluble bi-nitroxide, typically prepared in a 60/40 mixture of glycerol/water, whereas TEKPOL[8] is appropriate for organic solvents such as the TCE. Other exogenous radicals can be used, for instance, trityl, BDPA, paramagnetic ions (e.g., Gd(III) or Cr(III) complexes) or mixtures of radicals that can enable use of different DNP mechanisms in a single sample (not presented in this application note, see reference[9]).

The concentration of the polarizing agent is an important parameter to optimize. This will influence the efficiency of the DNP transfer, affecting both build-up time constant and ultimate polarization level that can be achieved. Also, with excessive radical concentrations spatial proximity of electron and nuclear spins may limit nuclear spin coherence lifetimes and quench NMR signals. Instead, optimizing the appropriate radical concentration can yield short build ups and a faster experimental recycle time. Typically, optimal radical concentrations are between 5 to 20 mM for bi-nitroxydes and cross-effect DNP at 100 K. However, values outside this range may benefit certain combinations of polarizing agent and sample.

Figure 1
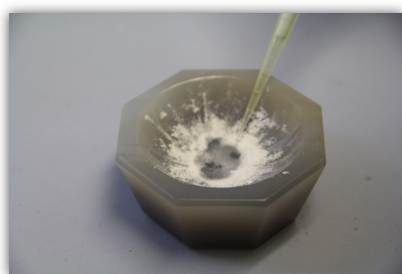
Picture 1

Picture 2

Picture 3

Figure 1: Preparation of a material sample for DNP using the impregnation method. The material (finely ground white powder) is (1) wetted with a solvent solution containing the dissolved radical, then (2) impregnation and a few minutes of manual mixing with a spatula, and, finally, (3) the sample is transferred into a MAS rotor for DNP analysis.

The deuteriation level of the solvent must also be considered. It enables control in the efficiency of proton spin diffusion, which is typically needed to distribute DNP-derived hyperpolarization throughout the sample. Properly optimized deuteration can be necessary for best the NMR sensitivity. Diminution of the number of protons in the sample mixture (often dominated by solvent) increases the nuclear relaxation time to allow higher ultimate polarization level in both the remaining proton spins, and in heteronuclei. Solvent mixtures of glycerol-d8/D_2O/H_2O (60/30/10, volume ratio), DMSO-d6/D_2O/H_2O (78/14/8) or TCE-d2/TCE (90/10) are typically used for initial DNP sample preparation.

For material samples containing an endogenous radical, DNP measurements can be performed directly on the native sample[10], without added solvent or radical. For best DNP, the matching condition between the nuclear and the electron frequencies may need to be adjusted relative to the standard default match for nitroxide (or bi-nitroxide) radicals. Adjustment is commonly performed by variation of the NMR field and frequency while the MW frequency remains constant (the so-called DNP field-sweep experiment). Obtaining an EPR spectrum of the material containing endogenous radical will provide essential information (electron g-factor or EPR frequency) to guide field-sweep conditions (range and center point over which DNP is optimized). In addition, EPR may be used to determine the radical concentration using the Spin Counting module (as available on Bruker ESR5000 and EMX Nano instruments). Figure 2 shows examples of EPR traces for various radicals used in DNP.

Finally, after suitable preparation from above, the material sample is packed into a MAS rotor (Figure 1). For 3.2 mm rotors, two types of rotor material can be used:

1) Sapphire: aluminum oxide (Al_2O_3) has a good permeability to MW radiation and good thermal conductivity for uniform sample cooling. For these reasons, sapphire rotors can yield higher DNP enhancement compared to rotors made with zirconium dioxide.

2) Zirconium dioxide: (zirconia, ZrO_2) especially used for investigation of samples with ^{27}Al, where sapphire would present a large background signal. Additionally, sapphire rotors are not available at the smallest rotor sizes (e.g., $\leq$ 1.9 mm diameter), whereas zirconia remains an excellent choice for DNP.

For both types of rotors, material selection for plug inserts and a top cap is also critical and must also account for low temperature (e.g., 100 K) compatibility. Top caps are typically of zirconia (ZrO_2). The top insert is usually made with Teflon for solvent impregnated material samples. For liquid samples silicone rubber is preferred to prevent solvent leaks (particularly for the glass-forming method). For smaller diameter ZrO_2 rotors (0.7, 1.3 and 1.9 mm), Vespel top and bottom caps are used. Operating at low temperature (ca. 100 K), a special set of rotor and caps are designed with tight fit of top and bottom Vespel caps. Bruker 1.3 and 1.9 mm rotors for DNP are provided with tight-fitting, specially paired Vespel mating parts.
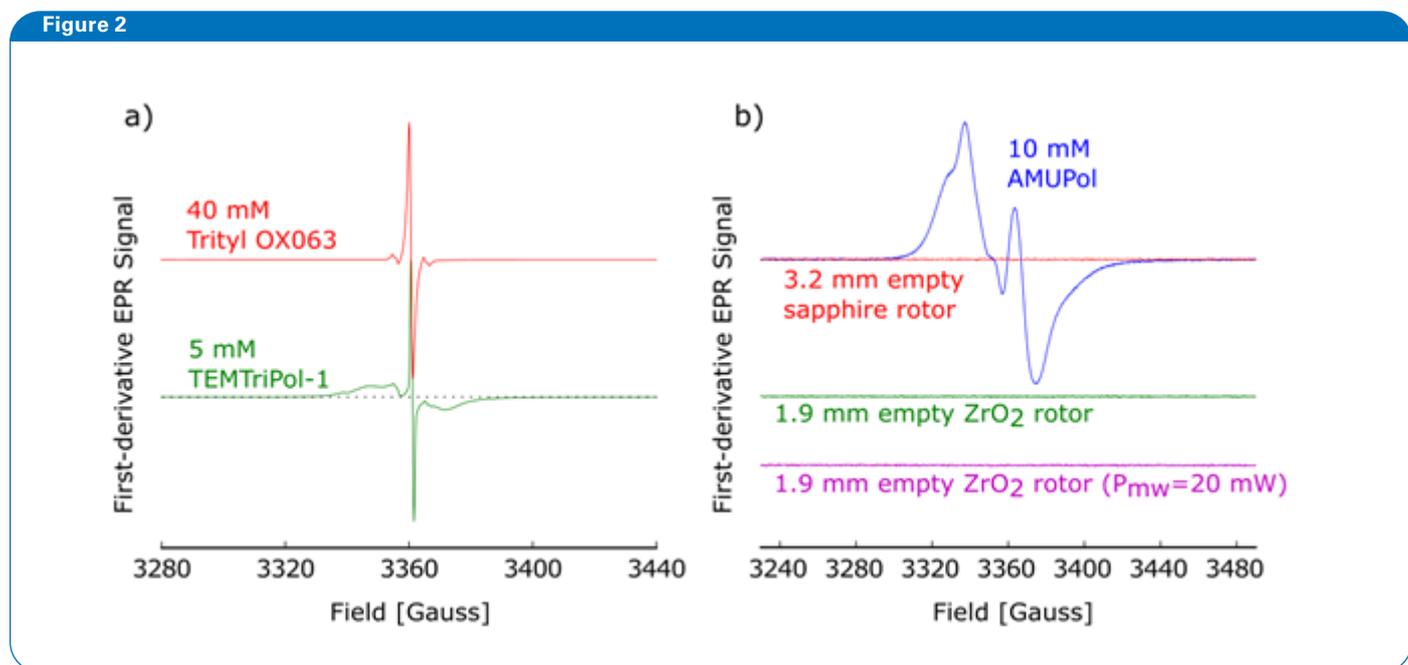
Figure 2

Figure 2: Room-temperature X-band EPR spectra of a) Trityl OX063, TEMTriPol-1 and b) AMUPol radicals acquired on a Bruker Magnettch ESR-5000 spectrometer. At the same measurement parameters, the sapphire and ZrO2 rotors show no perceivable EPR signals. The microwave power is 1 mW unless specified.

Figure 3 and Figure 4 show two examples of DNP experiments on commercial material samples. The sample preparation method, following above procedures, is described in the figure caption along with the resulting gain in NMR sensitivity with (DNP) and without (no DNP) MW irradiation at 263 GHz.

Figure 3 and 4

^{29}Si chemical shift (ppm)

^{27}Al chemical shift (ppm)

Figure 3: ^{29}Si CP-MAS NMR spectra of silica (Sigma-Aldrich, 2 μm particle size, ≈ 4 nm pore size) at 9.4 T and 8 kHz spinning frequency in 3.2 mm sapphire rotor. 30 mg of silica sample was impregnated with 15 μL of a solution containing 10 mM TEKPOL in tetrachloroethane (TCE). The spectra were recorded a) without and b) with MW irradiation. The number of scans is 128 for each spectrum. The DNP signal enhancement is Ɛ(on/off) = 30.

Figure 4: ^{27}Al CP-MAS NMR spectra of alumina sample (Goodfellow, maximum particle size 0.1 μm, 99.99 % gamma-alumina) at 9.4 T and 8 kHz spinning frequency in 3.2 mm ZrO$_2$ rotor30 mg of alumina was impregnated with 40 μL of 10 mM AMUPOL in DMSO-d6/D$_2$O/H$_2$O (78/14/8 volume ratio). The spectra were recorded a) without and b) with MW irradiation; the number of scans is respectively 256 and 16. The DNP signal enhancement is Ɛ(on/off) = 120, after adjustment scan ratio of 16.

Solid-state DNP instrumentation

Figure 5 is a schematic view of a Bruker solid-state DNP systems. The main components are: (1) a microwave (MW) source, (2) a transmission line as an enclosed, low-loss pathway from source to (3) a solid-state low-temperature (LT) MAS DNP NMR probe, and (4) a cooling system to achieve ca. 100 K temperature of the spinning, microwave irradiated sample[11, 12]. The DNP NMR probe is specially designed to include low-loss MW waveguide, elements for efficient MW coupling to the sample, and both insulation and components for 3-channel (Bearing, Drive and Variable Temperature) gas flows in LT MAS. Cooling of the gases is provided by a liquid nitrogen heat exchanger with automated refiling and temperature, pressure monitoring and controls, all coupled to an automated MAS controller for stable high-speed spinning (see below).

The most common MW source is a gyrotron: a high-vacuum tube, with electron gun whose beam traverses a special cavity in the plateau of a high-field cryogen-free superconducting magnet. This produces high-power cw microwaves (> 10 W) at frequencies of 263, 395, 527 or 593 GHz in current Bruker systems. These correspond to ^{1}H NMR frequencies of 400, 600, 800, and 900 MHz, respectively. At 263 GHz, Bruker recently introduced a more-compact and lower-cost Klystron microwave source with up to 5 W output power and 70-80 % DNP performance compared to the higher-power Gyrotron at this field (Figure 5b). Material applications of DNP (e.g., to Li$^+$ batteries[13]) have produced excellent results using either source.

The external microwave transmission line connects the gyrotron to the DNP MAS probe. This wave guide is corrugated to reduce microwave power losses along the line. The DNP MAS probe also has an internal corrugated waveguide through which the microwaves can travel and then with a radially irradiation of the spinning sample into the MAS stator.

LT-MAS DNP NMR probes are available for four different rotor diameters: 0.7, 1.3, 1.9 and 3.2 mm with corresponding maximum spinning frequencies of 65, 40, 25, and 15 kHz at 100 K and using nitrogen gas for Bearing, Drive and VT.* All Bruker MAS DNP probes have automatic insert/eject capability, without interruption to LT conditions. This is essential for efficient screening of materials samples, while the probe remains at low temperature. Current DNP probes are available in double- (H/X) or triple-resonance (H/X/Y) modes. The 3.2mm H/X/Y DNP LT-MAS probe is the most versatile and widely used for material studies. This double broad-banded probe allows the detection of a wide range of nuclei, including user-selected pairs of X/Y spins, e.g., ^{13}C/^{15}N, ^{31}P/^{13}C, ^{27}Al/^{29}Si, etc., chosen by straightforward swapping of supplied tuning inserts. A 3.2 mm double-resonance DNP probe optimized for low-gamma nuclei is also quite valuable for materials characterization (tuning range from ^{15}N down to ^{39}K).

Fast-spinning MAS DNP probes, especially the 1.3 mm rotor diameter, are complementary for analysis materials samples.

* LT spinning rates are significantly less (60-65%) than at room temperature due to increased viscosity of g N$_2$ near 100 K. Spinning with lower viscosity gasses (e.g., g-He) is known to compensate that effect but can be prohibitively expensive.
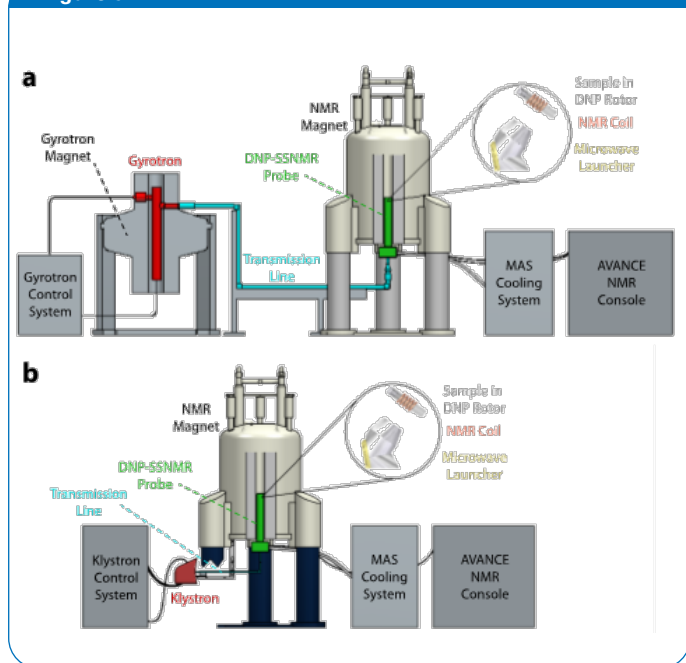
Figure 5: a) Schematic of a solid-state NMR DNP spectrometer with a gyrotron microwave source (gyrotron tube in red), a microwave transmission line (cyan) and a low-temperature MAS DNP probe (green). Currently Gyrotrons for DNP are available from Bruker at 263, 395 and 527 GHz (400, 600 and 800 MHz ^{1}H NMR frequencies), with one also currently installed at 593 GHz / 900 MHz b) For 263 GHz / 400 MHz, a more-compact and lower-cost klystron source is also available from Bruker.

The higher spinning frequency (up to 40 kHz at 1.3 vs. 15 kHz at 3.2 mm) offers higher spectral resolution and longer coherence lifetimes. These effects yield better DNP enhancement and detection sensitivity as well as lower losses and better resolution in multi-dimensional experiments. Moreover, for high-field DNP ($\geq$ 800 MHz ^{1}H frequency), enhancement factor is significantly better for the smaller-diameter rotors due to optimizations in coupling the MW irradiation to the smaller sample size[14]. Finally, more recently the introduction of 0.7 mm DNP probes and 800, 900 MHz may enable further gains in materials applications already witnessed with Bruker's 1.9 and 1.3 mm examples[15].

Finally, a key, but easily overlooked feature of the overall DNP system is the field-sweep capability of Bruker NMR magnets that are specially designated for DNP use. This consists of a superconducting sweep coil, permanently placed superconducting leads (and thermally controlled switch) and dedicated power supply. This feature is critical for investigation of a wide variety of polarizing agents, whose EPR (and hence DNP) frequencies may vary over >10,000 ppm. Field sweeping enables the DNP variety in spite of a (mostly) fixed-frequency MW source to detect direct X nuclei. The large frequency range is especially valuable in materials applications, where endogenous radicals are often quite distinct from the typically added (exogenous) radicals. (See detail on the chapter preparation of materials samples).

Materials studies by Solid-state DNP

Here, we present a selection of recent materials studies using DNP. Historically, high-field solid-state DNP NMR has been used mainly for study of biological samples, such as membranes proteins like bacteriorhodopsin and or aggregate assemblies like amyloid fibrils[16-18]. Starting especially in 2010, material applications were greatly stimulated by Lesage, et al. with DNP on mesoporous silica using radical impregnation[2]. This and several subsequent applications reviewed below demonstrate a new window opened to Materials Science by the ability of DNP to highlight previously inaccessible features, often buried in key regions of complex, structured samples.

The noted seminal study was applied to mesoporous silica functionalized on interior surfaces with small aromatic organics as well as trace quantities of various alkoxy species[19]. This work also introduced the impregnation method with addition of either mono- (TEMPO) or bi-radicals (TOTAPOL) in aqueous solution, as well as TEMPO in nonpolar solvent. Microwave irradiation near 263 GHz yielded ^{1}H enhancements in the solvent of (10 – 25)x depending on radical and solvent. ^{1}H spin-diffusion though the solvent plus CP yielded matching ^{13}C enhancements in the surface-attached species, including strong peaks assigned to the trace species. Subsequent works using this approach also allowed detection of natural-abundance ^{13}C, ^{29}Si and ^{15}N enhancements in surface-attached organics[20, 21]. The higher sensitivity has also enabled heteronuclear 2D NMR experiments (HETCOR ^{1}H/X, REDOR, etc.) to elucidate 3D structural features of the catalytic surface of an organometallic complex[22]. These achievements would not have been possible without DNP enhancement. Direct DNP of ^{29}Si has also been used to characterize the core of porous materials, whereas indirect enhancement (DNP of ^{1}H plus CP from ^{1}H to ^{29}Si) also revealed and enhances resonances from the surface of the material[23]. The surface active sites of amorphous aluminosilicates were also elucidated using the DNP approach with heteronuclear correlations experiments between ^{29}Si and ^{27}Al to determine atomic connectivities (through space and through bonds)[24].

The higher sensitivity from DNP also enabled the study of catalytic nanoparticle samples, meant to encompass materials with a size between 1 to 100 nanometers. Since 2015, many studies have been published using DNP to characterize such nanomaterials, including mesoporous alumina[25, 26], organo-silicates[27], nanocatalysts[28], supramolecular nanoassemblies[29], MOFs (Metal-Organic-Frameworks)[30], and metallic nanoparticles[31]. These various explored DNP-enhanced NMR for broad range of nuclei (^{13}C, ^{29}Si, ^{15}N, ^{27}Al, ^{119}Sn) using both homo- and heteronuclear 2D correlations experiments. DNP enhancement factors were notably high among these nanoscale systems, up to (10 – 100)x, corresponding to dramatic reductions of experiment times by (100 – 10,000)x.

Low-γ nuclei (typically meaning $\gamma \le \gamma$15N) are a frequent target of challenging questions in material samples. This was first demonstrated on inorganic solids (Mg(OH)$_2$) with ^{17}O at natural isotopic abundance[32]. Further studies with ^{17}O at natural abundance have characterized the surface features of silica gels and hydrogen-bonding dynamics of hydroxyls at the surface of mesoporous silica nanoparticles[33, 34]. These utilized ^{1}H-^{17}O PRESTO Q-CPMG experiments to identify various surface sites and reveal ^{1}H-^{17}O distances[35, 36]. This probed the Bronsted acidity of the surface hydroxyls as correlated with the pH at the zero point of charge in the materials. Direct ^{17}O DNP also made it possible to characterize the surface of nanoparticles and heterogeneous catalysts[37, 38].

High-field DNP can be especially advantageous with quadrupolar nuclei like ^{17}O, due to reduced second-order quadrupolar broadening, which scales as (1/B$_0$). Blanc and co-workers[39] took advantage of this at B$_0$ = 18.8 T (800 MHz ^{1}H frequency) on Mg(OH)$_2$ powder samples in a glassy formulation with BDPA radical in o-terphenyl solvent. This utilized Overhauser effect (OE) DNP to obtain 17x enhancement at ^{17}O after CP from direct DNP on ^{1}H in the solvent. The OE mechanism tends to scale more favorably with B0 vs. mechanisms (Cross-Effect, Solid-Effect) more typically used for DNP in 400 – 600 MHz NMR. However, the authors also utilized CE DNP with TEKPol radical, achieving only slightly lower enhancements of (9 – 14)x and providing an advantage of ~3x faster DNP buildup.

Another interesting target of low-γ DNP studies has been ^{89}Y (~19.6 MHz with a ^{1}H frequency at 400 MHz). Efficient enhancement by indirect DNP (^{1}H-^{89}Y CP MAS) has been obtained on hydrated Yttrium-doped barium zirconate (BaZrO$_3$) ceramics[40]. These are protonic conductors and promising targets as energy storage materials. The particular samples studied consisted of micron-scale particles (d < 45 µm and 45 µm < d < 75 µm) impregnated with AMUPol biradical in a frozen glassy matrix with H$_2$O/DMSO-d$_6$ (40/60), among other formulations tested. DNP enabled observation of ^{89}Y signals in only few minutes, whereas, even after several hours acquisition, no signal was observed without microwave irradiation. In addition, DNP-enhanced 2D ^{1}H ^{89}Y HETCOR spectra revealed additional chemical and conformational variety at yttrium sites. Altogether, DNP results analyzed in concert with DFT calculations allowed assignment and definition of different H-bonding states at local yttrium and proton sites. Resulting definition of functional features in the materials would not have been practical to obtain by NMR without DNP enhancements.

Another promising field for DNP application is the characterization of biomaterials. A key example is hydroxyapatite, a constituent of bone and teeth, as explored using DNP in a 2017 study by Lee, et al[41]. There, ^{43}Ca NMR (~27.0 MHz with a ^{1}H frequency at 400 MHz) was used to distinguish interfacial and core Ca^{2+} species in nanocrystalline (d ~ 30 nm) carbonated hydroxyapatites [C Hap = Ca$_{10}$(PO$_4$)$_6$(OH)$_2$], as well as to define interfacial environments of the cations. DNP samples were prepared by wetting C–HAp powder with 30 µl of 10 mM AMUPol in glycerol-d$_8$/D$_2$O/H$_2$O (60/30/10, v/v/v). DNP plus ^{1}H→^{43}Ca CP enabled rapid observation (<1 h) of 1D spectra at natural abundance (0.14% ^{43}Ca). Even more impressive, 2D 1H-^{43}Ca HETCOR experiments were acquired in only few hours, reported as the first ever without isotopic enrichment of ^{43}Ca. The 2D correlations distinguished Ca+ sites coordinated to OH– groups in columnar channels of nanoscale domains from those of surface OH– groups hydrogen-bonded to water or other surface-adsorbed solvents. The authors reported DNP gains not as the typical microwave on/off ratio of peak areas, but rather as absolute sensitivity ratio of ~35. This offer is a more conservative estimate of DNP gains, as the on/off ratio was calculated using an off spectrum from a more densely packed sample that was absent solvent additives used in the 'on' spectrum with DNP.

In another study, 2D (^{1}H,^{31}P), (^{31}P,^{13}C) and (^{13}C,^{13}C) HETCOR spectra with ^{1}H DNP plus CP transfers was used to assess complementary structural features of hydroxyapatites[42]. Meanwhile, other examples in the field of biomaterials include use of ^{13}C DNP to evaluate native collagen protein in skin and bones[43], further evidencing that the method is a new avenue to atomic-scale resolution of biomaterial structure/function relationships.

Synthetic polymers are another class of materials investigated by solid-state DNP, including in a variety of states (amorphous or semi-crystalline) and chemical compositions. With the development of Viel and coworkers, sample preparation methods have extensively tested across this variety to achieve highest NMR sensitivity[44, 45]. With these innovative approaches, DNP now makes it possible to detect the dilute end-chain signals from large synthetic polymers. This has been valuable to explore the living, active site of polymerization reactions and is playing an important role in development of so-called 'smart' materials.

We also mention the study of an organic semiconducting thin film using static solid-state DNP[46]. The properties of these devices, such as organic light emitting diodes (OLEDs), depend on the intra- and inter-molecular structures that could be characterized by static ssNMR. However, the amount of material is limited on thin film samples, resulting in poor sensitivity of detection by ssNMR. Using a static DNP probe, the authors analyzed one single glass plate, containing only 52 µg of thin film, to determine the phosphorus-oxygen bond (^{31}P=O) orientation within the sample. This innovative characterization method will enable more rational and efficient design of semiconductor thin films.

As a final example, one of the most exciting materials applications of DNP are recent studies of Li$^+$ and Li-metal battery materials by Leskes, Grey and coworkers[13, 47-50]. The solid electrolyte interface (SEI) is the critical functional region of rechargeable batteries and, buried between bulk anode and cathode regions, it is inherently challenging to study as a small contributor to overall signals. Performance and battery materials lifetime were analyzed by ^{13}C MAS-DNP at natural abundance. The increased sensitivity offered by MAS-DNP allowed detecting of organic species of the SEI in only a few hours. The selective observation of the SEI-metal interface has also been studied by ^7Li, ^1H and ^{19}F DNP solid-state NMR. Because of the sensitivity enhancement of one order of magnitude, it was possible to detect SEI species, revealing their chemical nature and spatial distribution. DNP studies using endogenous paramagnetic dopants in electrode materials were also recently investigated. Fe(III) metal ion dopant was incorporated into $Li_4Ti_5O_{12}$ materials yielding high lithium DNP enhancement (more than 100 for ^6Li). This new efficient metal ion DNP approach can be extended to the structural study of inorganic materials.

All these promising DNP results will contribute to a better understanding of the structure of complex materials for rechargeable batteries and the development of next generation high energy storage systems with an improved lifetime.

Conclusions

The examples in this application note demonstrate that the solid-state MAS DNP approach can be efficiently used to provide new insights for the structural characterization of a wide variety of materials. The NMR signal amplification offered by Dynamic Nuclear Polarization allows for the detection of dilute components within material samples and insensitive nuclei that would have been not possible by conventional solid-state NMR.

"Dedicated in honor and memory of Melanie Rosay, who not only contributed significantly to this writing but also for years inspired myself, many colleagues and collaborators in DNP NMR."

References

[1] Rankin, A. G. M.; Trébosc, J.; Pourpoint, F.; Amoureux, J.-P.; Lafon, O., Recent developments in MAS DNP-NMR of materials. Solid State Nuclear Magnetic Resonance 2019, 101, 116.

[2] Lesage, A.; Lelli, M.; Gajan, D.; Caporini, M. A.; Vitzthum, V.; Miéville, P.; Alauzun, J.; Roussey, A.; Thieuleux, C.; Mehdi, A.; Bodenhausen, G.; Coperet, C.; Emsley, L., Surface Enhanced NMR Spectroscopy by Dynamic Nuclear Polarization. Journal of the American Chemical Society 2010, 132, (44), 15459.

[3] Zagdoun, A.; Rossini, A. J.; Gajan, D.; Bourdolle, A.; Ouari, O.; Rosay, M.; Maas, W. E.; Tordo, P.; Lelli, M.; Emsley, L.; Lesage, A.; Coperet, C., Non-aqueous solvents for DNP surface enhanced NMR spectroscopy. Chem Commun (Camb) 2011, 48, (5), 654-6.

[4] Kubicki, D. J.; Rossini, A. J.; Purea, A.; Zagdoun, A.; Ouari, O.; Tordo, P.; Engelke, F.; Lesage, A.; Emsley, L., Amplifying Dynamic Nuclear Polarization of Frozen Solutions by Incorporating Dielectric Particles. Journal of the American Chemical Society 2014, 136, (44), 15711.

[5] Le, D.; Ziarelli, F.; Phan, T., N. T.; Mollica, G.; Thureau, P.; Aussenac, F.; Ouari, O.; Gigmes, D.; Tordo, P.; Viel, S., Up to 100% Improvement in Dynamic Nuclear Polarization Solid-State NMR Sensitivity Enhancement of Polymers by Removing Oxygen. Macromol. Rapid Commun. 2015, 36, 1416-1421.

[6] Hu, K. N.; Song, C.; Yu, H. H.; Swager, T. M.; Griffin, R. G., High-frequency dynamic nuclear polarization using biradicals: a multifrequency EPR lineshape analysis. J Chem Phys 2008, 128, (5), 052302.

[7] Sauvée, C.; Rosay, M.; Casano, G.; Aussenac, F.; Weber, R. T.; Ouari, O.; Tordo, P., Highly Efficient, Water-Soluble Polarizing Agents for Dynamic Nuclear Polarization at High Frequency. Angew. Chem. Int. Ed. 2013, 52, 1 – 5.

[8] Zagdoun, A.; Casano, G.; Ouari, O.; Schwarzwalder, M.; Rossini, A. J.; Aussenac, F.; Yulikov, M.; Jeschke, G.; Coperet, C.; Lesage, A.; Tordo, P.; Emsley, L., Large molecular weight nitroxide biradicals providing efficient dynamic nuclear polarization at temperatures up to 200 K. J Am Chem Soc 2013, 135, (34), 12790-7.

References

[9] Lilly Thankamony, A. S.; Wittmann, J. J.; Kaushik, M.; Corzilius, B., Dynamic nuclear polarization for sensitivity enhancement in modern solid-state NMR. Progress in Nuclear Magnetic Resonance Spectroscopy 2017, 102-103, 120.

[10] Riikonen, J.; Rigolet, S.; Marichal, C.; Aussenac, F.; Lalevée, J.; Morlet-Savary, F.; Fioux, P.; Dietlin, C.; Bonne, M.; Lebeau, B.; Lehto, V.-P., Endogenous Stable Radicals for Characterization of Thermally Carbonized Porous Silicon by Solid-State Dynamic Nuclear Polarization 13C NMR. J. Phys. Chem. C 2015, 119, 19272–19278.

[11] Rosay, M.; Blank, M.; Engelke, F., Instrumentation for solid-state dynamic nuclear polarization with magic angle spinning NMR. Journal of Magnetic Resonance 2016, 264, 88.

[12] Rosay, M.; Tometich, L.; Pawsey, S.; Bader, R.; Schauwecker, R.; Blank, M.; Borchard, P. M.; Cauffman, S. R.; Felch, K. L.; Weber, R. T.; Temkin, R. J.; Griffin, R. G.; Maas, W. E., Solid-state dynamic nuclear polarization at 263 GHz: spectrometer design and experimental results. Phys Chem Chem Phys 2010, 12, (22), 5850-60.

[13] Hope, M. A.; Rinkel, B. L. D.; Gunnarsdottir, A. B.; Märker, K.; Menkin, S.; Paul, S.; Sergeyev, I. V.; Grey, C. P., Selective NMR observation of the SEI-metal interface by dynamic nuclear polarisation from lithium metal. "Nature Communications" 2020, 11, (1), 2224.

[14] Chaudhari, S. R.; Wisser, D.; Pinon, A. C.; Berruyer, P.; Gajan, D.; Tordo, P.; Ouari, O.; Reiter, C.; Engelke, F.; Coperet, C.; Lelli, M.; Lesage, A.; Emsley, L., Dynamic Nuclear Polarization Efficiency Increased by Very Fast Magic Angle Spinning. Journal of the American Chemical Society 2017, 139, (31), 10609.

[15] Berruyer, P.; Björgvinsdottir, S.; Bertarello, A.; Stevanato, G.; Rao, Y.; Karthikeyan, G.; Casano, G.; Ouari, O.; Lelli, M.; Reiter, C.; Engelke, F.; Emsley, L., Dynamic Nuclear Polarization Enhancement of 200 at 21.15 T Enabled by 65 kHz Magic Angle Spinning. The Journal of Physical Chemistry Letters 2020, 11, (19), 8386.

[16] Bayro, M. J.; Debelouchina, G. T.; Eddy, M. T.; Birkett, N. R.; MacPhee, C. E.; Rosay, M.; Maas, W. E.; Dobson, C. M.; Griffin, R. G., Intermolecular Structure Determination of Amyloid Fibrils with Magic-Angle Spinning and Dynamic Nuclear Polarization NMR. Journal of the American Chemical Society 2011, 133, (35), 13967.

[17] Bajaj, V. S.; Mak-Jurkauskas, M. L.; Belenky, M.; Herzfeld, J.; Griffin, R. G., Functional and shunt states of bacteriorhodopsin resolved by 250 GHz dynamic nuclear polarization–enhanced solid-state NMR. Proc Natl Acad Sci U S A 2009, 106 (23), 9244-9249.

[18] Hall, D. A.; Maus, D. C.; Gerfen, G. J.; Inati, S. J.; Becerra, L. R.; Dahlquist, F. W.; Griffin, R. G., Polarization-Enhanced NMR Spectroscopy of Biomolecules in Frozen Solution. Science 1997, 276, (5314), 930.

[19] Gruning, W. R.; Rossini, A. J.; Zagdoun, A.; Gajan, D.; Lesage, A.; Emsley, L.; Coperet, C., Molecular-level characterization of the structure and the surface chemistry of periodic mesoporous organosilicates using DNP-surface enhanced NMR spectroscopy. Physical Chemistry Chemical Physics 2013, 15, (32), 13270.

[20] Kobayashi, T.; Lafon, O.; Lilly Thankamony, A. S.; Slowing, I. I.; Kandel, K.; Carnevale, D.; Vitzthum, V.; Vezin, H.; Amoureux, J.-P.; Bodenhausen, G.; Pruski, M., Analysis of sensitivity enhancement by dynamic nuclear polarization in solid-state NMR: a case study of functionalized mesoporous materials. Physical Chemistry Chemical Physics 2013, 15, (15), 5553.

[21] Lelli, M.; Gajan, D.; Lesage, A.; Caporini, M. A.; Vitzthum, V.; Mieville, P.; Heroguel, F.; Rascon, F.; Roussey, A.; Thieuleux, C.; Boualleg, M.; Veyre, L.; Bodenhausen, G.; Coperet, C.; Emsley, L., Fast characterization of functionalized silica materials by silicon-29 surface-enhanced NMR spectroscopy using dynamic nuclear polarization. J Am Chem Soc 2011, 133, (7), 2104-7.

[22] Berruyer, P.; Lelli, M.; Conley, M. P.; Silverio, D. L.; Widdifield, C. M.; Siddiqi, G.; Gajan, D.; Lesage, A.; Coperet, C.; Emsley, L., Three-Dimensional Structure Determination of Surface Sites. Journal of the American Chemical Society 2016, 139, (2), 849.

[23] Lafon, O.; Rosay, M.; Aussenac, F.; Lu, X.; Trebosc, J.; Cristini, O.; Kinowski, C.; Touati, N.; Vezin, H.; Amoureux, J. P., Beyond the Silica Surface by Direct Silicon-29 Dynamic Nuclear Polarization. Angew Chem Int Ed Engl 2011, 50, 1-5.

References

[24] Valla, M.; Rossini, A. J.; Caillot, M.; Chizallet, C.; Raybaud, P.; Digne, M.; Chaumonnot, A.; Lesage, A.; Emsley, L.; van Bokhoven, J. A.; Copéret, C., Atomic Description of the Interface between Silica and Alumina in Aluminosilicates through Dynamic Nuclear Polarization Surface-Enhanced NMR Spectroscopy and First-Principles Calculations. Journal of the American Chemical Society 2015, 137, (33), 10710.

[25] Kobayashi, T.; Perras, F. A.; Slowing, I. I.; Sadow, A. D.; Pruski, M., Dynamic Nuclear Polarization Solid-State NMR in Heterogeneous Catalysis Research. ACS Catalysis 2015, 5, (12), 7055.

[26] Lafon, O.; Thankamony, A. S. L.; Kobayashi, T.; Carnevale, D.; Vitzthum, V.; Slowing, I. I.; Kandel, K.; Vezin, H.; Amoureux, J.-P.; Bodenhausen, G.; Pruski, M., Mesoporous Silica Nanoparticles Loaded with Surfactant: Low Temperature Magic Angle Spinning 13C and 29Si NMR Enhanced by Dynamic Nuclear Polarization. The Journal of Physical Chemistry C 2013, 117, (3), 1375.

[27] Lee, D.; Takahashi, H.; Thankamony, A. S. L.; Dacquin, J.-P.; Bardet, M.; Lafon, O.; de Paëpe, G., Enhanced Solid-State NMR Correlation Spectroscopy of Quadrupolar Nuclei Using Dynamic Nuclear Polarization. Journal of the American Chemical Society 2012, 134, (45), 18491.

[28] Lee, D.; Monin, G.; Duong, N. T.; Lopez, I. Z.; Bardet, M.; Mareau, V.; Gonon, L.; De Paëpe, G., Untangling the Condensation Network of Organosiloxanes on Nanoparticles using 2D 29Si-29Si Solid-State NMR Enhanced by Dynamic Nuclear Polarization. Journal of the American Chemical Society 2014, 136, (39), 13781.

[29] Marker, K.; Paul, S.; Fernandez-de-Alba, C.; Lee, D.; Mouesca, J.-M.; Hediger, S.; De Paepe, G., Welcoming natural isotopic abundance in solid-state NMR: probing [small pi]-stacking and supramolecular structure of organic nanoassemblies using DNP. Chemical Science 2017, 8, (2), 974.

[30] Rossini, A. J.; Zagdoun, A.; Lelli, M.; Canivet, J.; Aguado, S.; Ouari, O.; Tordo, P.; Rosay, M.; Maas, W. E.; Copéret, C.; Farrusseng, D.; Emsley, L.; Lesage, A., Dynamic Nuclear Polarization Enhanced Solid-State NMR Spectroscopy of Functionalized Metal–Organic Frameworks. Angewandte Chemie International Edition 2012, 51, (1), 123.

[31] Protesescu, L.; Rossini, A. J.; Kriegner, D.; Valla, M.; de Kergommeaux, A.; Walter, M.; Kravchyk, K. V.; Nachtegaal, M.; Stangl, J.; Malaman, B.; Reiss, P.; Lesage, A.; Emsley, L.; Copéret, C.; Kovalenko, M. V., Unraveling the Core-Shell Structure of Ligand-Capped Sn/SnOx Nanoparticles by Surface-Enhanced Nuclear Magnetic Resonance, Mössbauer, and X-ray Absorption Spectroscopies. ACS Nano 2014, 8, (3), 2639.

[32] Blanc, F. d. r.; Sperrin, L.; Jefferson, D. A.; Pawsey, S.; Rosay, M.; Grey, C. P., Dynamic Nuclear Polarization Enhanced Natural Abundance 17O Spectroscopy. Journal of the American Chemical Society 2013, 135, (8), 2975.

[33] Perras, F. A.; Chaudhary, U.; Slowing, I. I.; Pruski, M., Probing Surface Hydrogen Bonding and Dynamics by Natural Abundance, Multidimensional, 17O DNP-NMR Spectroscopy. The Journal of Physical Chemistry C 2016, 120, (21), 11535.

[34] 34. Perras, F. A.; Kobayashi, T.; Pruski, M., Natural Abundance 17O DNP Two-Dimensional and Surface-Enhanced NMR Spectroscopy. Journal of the American Chemical Society 2015, 137, (26), 8336.

[35] Perras, F. A.; Boteju, K. C.; Slowing, I. I.; Sadow, A. D.; Pruski, M., Direct 17O dynamic nuclear polarization of single-site heterogeneous catalysts. Chemical Communications 2018, 54, (28), 3472.

[36] Perras, F. A.; Wang, Z.; Naik, P.; Slowing, I. I.; Pruski, M., Natural Abundance 17O DNP NMR Provides Precise O-H Distances and Insights into the Brönsted Acidity of Heterogeneous Catalysts. Angewandte Chemie International Edition 2017, 56, (31), 9165.

[37] Li, W.; Wang, Q.; Xu, J.; Aussenac, F.; Qi, G.; Zhao, X.; Gao, P.; Wang, C.; Deng, F., Probing the surface of gamma-Al2O3 by oxygen-17 dynamic nuclear polarization enhanced solid-state NMR spectroscopy. Physical Chemistry Chemical Physics 2018, 20, (25), 17218-17225.

[38] Hope, M. A.; Halat, D. M.; Magusin, P. C. M. M.; Paul, S.; Peng, L.; Grey, C. P., Surface-selective direct 17O DNP NMR of CeO2 nanoparticles. Chemical Communications 2017, 53, (13), 2142.

[39] Brownbill, N. J.; Gajan, D.; Lesage, A.; Emsley, L.; Blanc, F., Oxygen-17 dynamic nuclear polarisation enhanced solid-state NMR spectroscopy at 18.8 T. Chemical Communications 2017, 53, (17), 2563.

References

[40] Blanc, F.; Sperrin, L.; Lee, D.; Dervisoglu, R.; Yamazaki, Y.; Haile, S. M.; De Paëpe, G.; Grey, C. P., Dynamic Nuclear Polarization NMR of Low-gamma Nuclei: Structural Insights into Hydrated Yttrium-Doped BaZrO3. The Journal of Physical Chemistry Letters 2014, 5, (14), 2431.

[41] Lee, D.; Leroy, C.; Crevant, C.; Bonhomme-Coury, L.; Babonneau, F.; Laurencin, D.; Bonhomme, C.; De Paëpe, G., Interfacial Ca2+ environments in nanocrystalline apatites revealed by dynamic nuclear polarization enhanced 43Ca NMR spectroscopy. "Nature Communications" 2017, 8, 14104.

[42] Leroy, C.; Aussenac, F.; Bonhomme-Coury, L.; Osaka, A.; Hayakawa, S.; Babonneau, F.; Coelho-Diogo, C.; Bonhomme, C., Hydroxyapatites: Key Structural Questions and Answers from Dynamic Nuclear Polarization. Analytical Chemistry 2017, 89, (19), 10201-10207.

[43] Singh, C.; Rai, R. K.; Aussenac, F.; Sinha, N., Direct Evidence of Imino Acid-Aromatic Interactions in Native Collagen Protein by DNP-Enhanced Solid-State NMR Spectroscopy. J. Phys. Chem. Lett. 2014, 5, 4044–4048.

[44] Le, D.; Casano, G.; Phan, T., N. T.; Ziarelli, F.; Ouari, O.; Aussenac, F.; Thureau, P.; Mollica, G.; Gigmes, D.; Tordo, P.; Viel, S., Optimizing Sample Preparation Methods for Dynamic Nuclear Polarization Solid-state NMR of Synthetic Polymers. Macromolecules 2014, 47, 3909–3916.

[45] Ouari, O.; Phan, T.; Ziarelli, F.; Casano, G.; Aussenac, F.; Thureau, P.; Gigmes, D.; Tordo, P.; Viel, S. p., Improved Structural Elucidation of Synthetic Polymers by Dynamic Nuclear Polarization Solid-State NMR Spectroscopy. ACS Macro Lett. 2013, 2, 715–719.

[46] Suzuki, K.; Kubo, S.; Aussenac, F.; Engelke, F.; Fukushima, T.; Kaji, H., Analysis of Molecular Orientation in Organic Semiconducting Thin Films Using Static Dynamic Nuclear Polarization Enhanced Solid-State NMR Spectroscopy. Angewandte Chemie International Edition 2017, 56, (47), 14842-14846.

[47] Harchol, A.; Reuveni, G.; Ri, V.; Thomas, B.; Carmieli, R.; Herber, R. H.; Kim, C.; Leskes, M., Endogenous Dynamic Nuclear Polarization for Sensitivity Enhancement in Solid-State NMR of Electrode Materials. The Journal of Physical Chemistry C 2020, 124, (13), 7082.

[48] Leskes, M.; Kim, G.; Liu, T.; Michan, A. L.; Aussenac, F.; Dorffer, P.; Paul, S.; Grey, C. P., Surface-Sensitive NMR Detection of the Solid Electrolyte Interphase Layer on Reduced Graphene Oxide. The Journal of Physical Chemistry Letters 2017, 8, (5), 1078-1085.

[49] Jin, Y.; Kneusels, N.-J. H.; Magusin, P. C. M. M.; Kim, G.; Castillo-Martinez, E.; Marbella, L. E.; Kerber, R. N.; Howe, D. J.; Paul, S.; Liu, T.; Grey, C. P., Identifying the Structural Basis for the Increased Stability of the Solid Electrolyte Interphase Formed on Silicon with the Additive Fluoroethylene Carbonate. Journal of the American Chemical Society 2017, 139, (42), 14992.

[50] Haber, S.; Leskes, M., Dynamic Nuclear Polarization in battery materials. "Solid State Nuclear Magnetic Resonance" 2021, 117, 101763.

● **Bruker BioSpin**

info@bruker.com
www.bruker.com